HHS Public Access

Author manuscript

Nat Immunol. Author manuscript; available in PMC 2014 June 01.

Published in final edited form as:

Nat Immunol. 2013 December ; 14(12): 1266–1276. doi:10.1038/ni.2741.

mTOR modulates the antibody response to provide cross-protective immunity to lethal influenza infections

Rachael Keating[1], **Tomer Hertz**[2], **Marie Wehenkel**[1], **Tarsha L. Harris**[1], **Benjamin A. Edwards**[1], **Jennifer L. McClaren**[1], **Scott A. Brown**[1], **Sherri Surman**[3], **Zachary S. Wilson**[2], **Philip Bradley**[2], **Julia Hurwitz**[3], **Hongbo Chi**[1], **Peter C. Doherty**[1], **Paul G. Thomas**[1], and **Maureen A. McGargill**[1,4]

[1]Immunology, St. Jude Children's Research Hospital, Memphis, TN

[2]Vaccine and Infectious Disease Division, Fred Hutchinson Cancer Research Center, Seattle, WA

[3]Infectious Diseases, St. Jude Children's Research Hospital, Memphis, TN

Abstract

Highly pathogenic avian influenza viruses pose a continuing global threat. Current vaccines will not protect against novel pandemic viruses. Creating "universal" vaccines has been unsuccessful because the immunological mechanisms promoting heterosubtypic immunity are incompletely defined. We show that rapamycin, an immunosuppressive drug that inhibits mTOR, promotes cross-strain protection against lethal H5N1 and H7N9 infections when administered during H3N2 virus immunization. Rapamycin reduced germinal center formation and inhibited B cell class-switching, yielding a unique repertoire of antibodies that mediated heterosubtypic protection. Our data establish a requirement for mTORC1 in B cell class-switching and demonstrate that rapamycin skews the antibody response away from high affinity variant epitopes, targeting more conserved elements of hemagglutinin. These findings have intriguing implications for influenza vaccine design.

Introduction

Influenza A viruses infect a broad range of avian and mammalian species, cause high rates of morbidity and mortality, and kill over 250,000 people each year. The emergence of highly pathogenic H5N1 avian strains poses a serious threat for a deadly pandemic[1]. These viruses are endemic in poultry in Asia, Europe, and Africa. The reported 59% mortality rate in the 610 confirmed human H5N1cases gives obvious cause for concern (www.who.int/csr/disease/avian_influenza). Thus far, the H5N1 viruses have not transmitted efficiently

[4]To whom correspondence should be addressed, maureen.mcgargill@stjude.org.

Author contributions

R.K. and M.A.M. designed experiments, conducted experiments, analyzed data, and wrote the paper. P.C.D. and P.G.T. designed experiments, contributed reagents, and edited the manuscript. J.L.M. conducted experiments and analyzed data. T.H., M.W., T.L.H., S.A.B., and B.A.E. designed experiments, conducted experiments, analyzed data, and commented on the manuscript. S.S., Z.S.W., and P.B. conducted experiments and analyzed data. J.H. and H.C. designed experiments and contributed reagents.

between people. However, influenza viruses change constantly, and as few as five mutations in an avian H5N1 virus enabled its aerosol transmission in ferrets[2,3]. Ferrets are generally considered a surrogate for human spread, indicating that virulent H5N1 variants could emerge and cause a severe pandemic.

Vaccination is the most effective strategy for controlling the spread of influenza, however, current vaccines have several limitations[4]. Most notably, existing vaccines do not provide strong heterosubtypic immunity, which is defined as protection against multiple subtypes of influenza. These virus subtypes are based on expression of the highly variable hemagglutinin (H or HA) and neuraminidase (N or NA) surface proteins. Pressure from the host immune response drives selection of HA and NA mutants that escape neutralization. Consequently, current vaccines do not protect against continuously emerging strains that present as variants of circulating “seasonal” viruses. Moreover, existing vaccines do not protect against pandemic viruses that arise from reassortment of influenza gene segments between different strains, which leads to the emergence of HA and NA subtypes that are novel in human populations. Despite extensive surveillance of both human and animal influenza viruses, it is difficult to predict which variants of HA and NA might acquire epidemic or pandemic potential.

Another limitation of current vaccines is that they are made in embryonated hen’s eggs. Production can be greatly limited if highly pathogenic strains are lethal for chick embryos, which occurs with some avian H5N1 strains[4]. Even when the production is straightforward, virus isolation to product availability generally takes at least six months, a delay that could cost millions of lives in the event of a new pandemic caused by these rapidly spreading pathogens.

A “universal” vaccine that induces immunity to conserved epitopes expressed in all influenza A virus subtypes could protect against novel strains, including highly virulent pandemic strains[4]. However, the immunological mechanisms that underlie the generation of such cross-reactive, heterosubtypic immune responses are poorly characterized, and attempts to generate broadly protective vaccines have had very limited success thus far[4]. The majority of epitopes conserved between different subtypes of influenza are from components internal to the virus, which limits their access for antibody neutralization. However, both $CD8^+$ and $CD4^+$ T cells contribute to viral clearance by recognizing influenza peptides from internal proteins[5]. While virus-specific memory T cells do not prevent viral entry into epithelial cells in the same manner as neutralizing antibodies, these cells decrease influenza-related morbidity and mortality by eliminating infected cells and accelerating viral clearance. Moreover, after considerable effort, cross-reactive antibodies specific for HA epitopes conserved between different influenza subtypes have been identified[6–13]. However, these “broad spectrum” B cell clones are extremely rare. Thus, a means to boost the memory T and B cell responses following influenza vaccination clearly merits extensive investigation as it may enhance protection against newly emerging viruses with the potential to create deadly pandemics.

Recently, several groups demonstrated that inhibiting mTOR by rapamycin treatment enhanced the generation of memory $CD8^+$ T cells. mTOR is a serine-threonine kinase that

responds to changes in the cellular environment, and in turn, regulates cell survival, metabolism, and proliferation[14]. Given that rapamycin is an immunosuppressive drug that blocks the proliferation and migration of B and T lymphocytes, it is surprising that rapamycin also enhances the generation of memory $CD8^+$ T cells. This was first demonstrated following the infection of mice with lymphocytic choriomeningitis virus (LCMV) and *Listeria monocytogenes*[15,16]. Subsequently, rapamycin was shown to increase memory cells following vaccinia virus infection in nonhuman primates[17], priming of mice with a heat shock protein-based cancer vaccine[18], and *in vitro* stimulation with peptide and antigen presenting cells[19]. Rapamycin increases both the number of memory $CD8^+$ T cells and the proportion with a long-lived memory phenotype ($CD127^{hi}$ $CD62L^{hi}$ $Bcl2^{hi}$ and $KLRG1^{lo}$). However, it is not clear whether this enhanced memory generation improves protection following a secondary infection. In addition, the jury is out on whether an enhanced immune response will protect against a lethal, heterosubtypic influenza infection without exacerbating immunopathology and mortality.

We show here that rapamycin treatment during primary H3N2 virus infection protects mice against a lethal, heterosubtypic, secondary H5N1 virus infection. Consequently, we utilized this system to investigate the components of the immune response critical for this protection. Surprisingly, the $CD8^+$ memory T cells were not required, though $CD4^+$ T cells and B cells were essential. Rapamycin treatment reduced B cell class-switching and altered the pattern of IgG and IgM specificities, yielding a unique antibody repertoire. In addition, transfer of serum was sufficient to protect naïve mice against a lethal H5N1 infection. Together, these data suggest that mTOR promotes B cell class-switching to generate a repertoire of high affinity, class-switched antibodies that protect against subsequent infections with the same virus, while reducing the frequency of antibodies potentially cross-reactive to conserved epitopes. Thus, current attempts to enhance immunity against conserved epitopes of universal vaccines may actually decrease the frequency of cross-reactive antibodies, hence reducing their capacity for heterosubtypic protection.

Results

Rapamycin protects against lethal H5N1 infection

To investigate whether low dose rapamycin treatment enhances vaccination efficacy to a pathogenic strain of influenza of a different subtype, mice were infected intraperitoneally (i.p.) with 1×10^8 EID_{50} of the A/HK/x31 (HKx31, H3N2) influenza A virus and treated with 75 μg/kg of rapamycin daily for 28 days, beginning one day prior to infection (Supplemental Fig. 1). Given i.p., the HKx31 virus undergoes a defective growth cycle, producing the full spectrum of virus proteins but no infectious virus, similar to a vaccine[20,21]. After 28 days, mice were then infected intranasally (i.n.) with 4.5×10^5 EID_{50} of the ΔVn1203 (H5N1) virus. The ΔVn1203 strain is a recombinant virus that expresses the internal genes of A/Puerto Rico/8/34 (PR8) and the surface H5 and N1 glycoproteins from the virulent A/Vietnam/1203/04 strain. In addition, the polybasic cleavage site in the ΔVn1203 H5 was modified to restrict cleavage to trypsin-like proteases and enable its use in a BSL2 facility. This engineered ΔVn1203 virus causes a lethal infection at relatively low doses in mice[22]. Remarkably, daily treatment with rapamycin versus PBS during the

primary HKx31 infection dramatically increased the proportion of mice that survived a secondary infection with ΔVn1203 virus (Fig. 1a). Mice given rapamycin lost less weight (Fig. 1b) and cleared virus faster than the controls (Fig. 1c). Thus, rapamycin treatment during virus priming enhanced protection against a lethal, heterosubtypic influenza infection.

Since HKx31 undergoes a defective growth cycle when administered i.p., it elicits an immune response similar to a vaccine. Nevertheless, we also tested whether rapamycin would protect mice following i.n. infection with a live-attenuated influenza virus (LAIV) that models i.n. vaccines such as FluMist. Mice were treated with rapamycin one day prior to i.n. infection with 10^6 $TCID_{50}$ of a temperature-sensitive strain of HKx31, $HKx31_{ts}$[23]. Rapamycin treatment was continued for 28 days, at which time mice were challenged with ΔVn1203. Mice treated with rapamycin lost less weight following challenge with ΔVn1203 than mice given PBS (Supplementary Fig. 2). Together, these data demonstrate that rapamycin enhanced protection from a lethal H5N1 infection when administered during a primary i.n. infection with LAIV or i.p. infection with a virus of a different subtype.

Rapamycin protects against multiple influenza subtypes

We next examined whether rapamycin treatment would also protect mice against a lethal infection with other subtypes of influenza. Mice were infected i.p. with HKx31, treated with rapamycin daily, and challenged i.n. with either A/Anhui/1/2013, which is a novel H7N9 isolate obtained from a patient during the recent outbreak in China[24–26], or PR8, which is an H1N1 strain. Remarkably, mice infected with HKx31 and treated with rapamycin exhibited significantly improved survival rates following both H7N9 and PR8 infection compared to mice treated with PBS (Fig. 2a,b). Mice receiving rapamycin also lost less weight than PBS-treated mice following infection with the H7N9 strain (Supplementary Fig. 3a). Thus, protection mediated by rapamycin treatment during primary influenza infection is not limited to the H5N1 subtype, and extends to viruses of at least 3 different subtypes. Moreover, the H7N9 strain does not contain the same internal genes as the laboratory strains, making this protection even more noteworthy

Rapamycin-mediated protection requires virus priming

To determine whether a primary infection is required for the rapamycin-mediated protection against a lethal secondary infection, mice were treated with rapamycin for 28 days and infected with ΔVn1203 virus in the absence of a primary infection. We found that treatment with rapamycin without concurrent HKx31 virus exposure left mice fully susceptible to the lethal ΔVn1203 infection (Fig. 3a and Supplementary Fig. 3c), suggesting that rapamycin protects by modulating the primary immune response. To confirm that rapamycin did not alter the capacity of virus to infect or replicate in epithelial cells, lung virus titers were analyzed daily after infection with ΔVn1203 virus in the presence of rapamycin. Lung titers immediately after ΔVn1203 infection were comparable for rapamycin and PBS-treated, unprimed mice (Fig. 3b), indicating that rapamycin does not directly limit virus entry or replication. To examine whether rapamycin-mediated protection is antigen-specific, mice were infected with HKx31 virus, treated with PBS or rapamycin daily, and challenged with Sendai virus, a parainfluenza type 1 virus that does not cross-react with influenza. As a

control, mice that were not infected with HKx31 virus were also treated with PBS or rapamycin and infected with Sendai virus. Mice treated with either PBS or rapamycin, regardless of prior HKx31 infection, were not protected from a lethal Sendai virus infection (Fig. 3c and Supplementary Fig. 3d). Together, these data confirm that the protection provided by rapamycin is due to antigen-specific alterations in the primary immune response to the H3N2 virus.

CD8$^+$ T cells are dispensable for protection

Given that rapamycin treatment increased the number and quality of memory CD8$^+$ T cells in other models of infection[15–19], we examined whether rapamycin enhances influenza-specific CD8$^+$ T cell memory. Mice were infected with the HKx31 virus and treated with rapamycin or PBS for 27 days. At this time, a sample of blood was taken from each mouse, and the number of influenza-specific T cells was measured by analysis of tetramer binding. Compared to the PBS control, rapamycin treatment significantly increased the number of H-2D^b NP$_{366}$ or H-2D^b PA$_{224}$-specific memory T cells (Fig. 4a), and a greater proportion of these cells had a memory precursor CD127^{hi} KLRG1^{lo} phenotype (Supplementary Fig. 4). Moreover, five days following secondary infection with ΔVn1203 virus, the number of influenza-specific T cells in the spleen and bronchoalveolar lavage (BAL) was higher in mice treated with rapamycin compared to controls (Fig. 4b). These data show that, similar to LCMV and *Listeria* infection, rapamycin increases the number and quality of memory CD8$^+$ T cells following an influenza virus infection.

To test whether this increase in influenza-specific memory CD8$^+$ T cells is responsible for the enhanced protection, mice were immunized with a genetically modified HKx31 virus, ΔCD8-HKx31. This virus lacks the five dominant epitopes recognized by influenza-specific CD8$^+$ T cells and does not induce substantial populations of effector or memory CD8$^+$ T cells[27]. Mice were infected i.p. with ΔCD8-HKx31 virus, treated with rapamycin or PBS for 28 days, and then challenged i.n. with ΔVn1203 virus. Prior to the ΔVn1203 infection, a blood sample was taken and stained with influenza-specific tetramers, confirming that infection with ΔCD8-HKx31 virus did not generate memory CD8$^+$ T cells specific for H-2D^b NP, H-2D^b PA, H-2K^b PB1, or H-2D^b PB1-F2 (data not shown). In the absence of a significant number of CD8$^+$ T cell memory, treatment with rapamycin following ΔCD8-HKx31 virus infection still protected mice against a lethal ΔVn1203 challenge (Fig. 4c and Supplementary Fig. 3e). This suggests that memory CD8$^+$ T cells are not required for rapamycin-mediated protection. As infection with ΔCD8-HKx31 virus may have generated memory CD8$^+$ T cells specific for other viral epitopes not detected with tetramers, we confirmed the lack of requirement for memory CD8$^+$ T cells by depleting with anti-CD8 (53-6.7) antibody at 1 and 3 days prior to, and 1, 3, 5, and 17 days following HKx31 infection. Mice were also treated with rapamycin or PBS for 28 days, and then infected with ΔVn1203 virus. Analysis of blood just prior to ΔVn1203 infection showed that the anti-CD8 antibody effectively decreased the number of memory CD8$^+$ T cells to a pre-immune amount (Supplementary Fig. 5a,b). Again, in the absence of significant numbers of memory CD8$^+$ T cells, treatment with rapamycin following HKx31 infection enhanced protection against a lethal H5N1 infection (Fig. 4d). Together these data demonstrate that, although

rapamycin increased the number and quality of memory $CD8^+$ T cells, these effectors were not required for the enhanced protection provided by rapamycin.

$CD4^+$ T cells are required for protection

Given that $CD8^+$ T cells do not mediate this heterosubtypic protection, we tested whether $CD4^+$ T cells were involved by depleting with anti-CD4 (GK1.5) antibody, given 1 and 3 days prior to the primary infection, and 2, 5, 22, and 24 days following the HKx31 infection. Depletion of $CD4^+$ T cells through the priming period significantly abrogated the protection afforded by rapamycin treatment (Fig. 5a and Supplementary Fig. 3g). To further examine whether the $CD4^+$ T cells are required during the primary versus the secondary infection, the $CD4^+$ T cells were depleted either during the early phase of the primary response (days −3, −1, 2, and 5) or just prior to the secondary infection (days 22 and 24). Eliminating the $CD4^+$ T cells just prior to the secondary infection did not diminish the rapamycin-mediated protection (Fig. 5b and Supplementary Fig. 3h). By contrast, depletion during the primary response completely abolished this protection (Fig. 5c and Supplementary Fig. 3i). These data clearly show that $CD4^+$ T cells are required during the primary immune response against the H3N2 virus to establish rapamycin-mediated protection against a subsequent heterosubtypic, H5N1 infection.

We next tested the duration of rapamycin treatment needed to protect against a ΔVn1203 infection. Mice were infected with the HKx31 virus and given rapamycin or PBS for 5–28 days. Twenty-eight days following the primary infection, mice were challenged with the ΔVn1203 virus. We found that 20 days of rapamycin sufficiently protected mice from a lethal ΔVn1203 challenge, while 5 days of rapamycin did not increase survival (Fig. 5d and Supplementary Fig. 3j). Ten and 15 days of rapamycin provided partial protection. Together these data indicate that rapamycin is required during the first 15–20 days following a primary H3N2 infection to limit the consequences of an otherwise lethal, heterosubtypic, influenza A virus infection by a $CD4^+$ T-dependent process.

As inhibition of mTOR increases the number of regulatory T cells *in vivo* and *in vitro*[14], rapamycin may protect against a lethal H5N1 infection by promoting the number of regulatory T cells. However, compared to controls, we found no increase in the number or proportion of $Foxp3^+$ $CD25^+$ regulatory T cells initially after the primary infection (Supplementary Fig. 6a–b). In fact, the proportion and number of regulatory T cells in the blood 26 days after the primary infection was slightly decreased in mice treated with rapamycin compared to PBS (Supplementary Fig. 6c–d). Furthermore, the proportion or number of regulatory T cells in the spleen, BAL, or draining lymph nodes, 5 days after the secondary infection was similar between rapamycin and PBS-treated mice (Supplementary Fig. 6e–f), suggesting that protection against a lethal, heterosubtypic influenza infection does not require an increase in regulatory T cells.

B cells are required for protection

The fact that rapamycin is required during the first 15 days following the primary infection, yet provides protection 28 days later in a $CD4^+$ T cell-dependent manner, suggests that rapamycin may limit a secondary infection by altering the antibody response. If this is true,

rapamycin treatment during the primary infection should provide lasting protection beyond 28 days. To explore this possibility, mice were infected with HKx31 virus, treated with rapamycin or PBS daily for 28 days, and then challenged with ΔVn1203 virus 6 weeks later. A significantly greater proportion of mice treated with rapamycin survived the secondary infection compared to those treated with PBS despite the 6 week lag between rapamycin treatment and secondary infection (Fig. 6a and Supplementary Fig. 3k), suggesting that rapamycin provides durable protection. Next, to examine whether rapamycin provided protection by altering the generation of antibodies, we infected wildtype or B cell-deficient (μMT) mice with the HKx31 virus, treated the mice with rapamycin or PBS, and challenged with ΔVn1203 virus. We found that rapamycin did not protect μMT mice from a secondary ΔVn1203 infection (Fig. 6b), establishing that B cells are required for this antigen-dependent, rapamycin-mediated protection. Furthermore, if rapamycin protects against a lethal ΔVn1203 infection by modulating the antibody response during primary HKx31 infection, then antibodies generated during HKx31 priming in the presence of rapamycin should transfer protection to naïve mice challenged with the lethal dose of ΔVn1203 virus. Thus, serum from mice infected with HKx31 virus and treated with rapamycin or PBS was transferred into naïve μMT mice one day prior to i.n. infection with ΔVn1203 virus. The controls received serum from naïve mice or mice previously infected with ΔVn1203 virus. Remarkably, similar to mice given serum from ΔVn1203-immune mice, the mice that received serum from rapamycin-treated mice infected with the HKx31 virus were also protected from a lethal ΔVn1203 infection, while mice that received serum from naïve mice or HKx31-infected PBS-treated mice were not protected (Fig. 6c and Supplementary Fig. 3l). These data suggest that rapamycin treatment protects against a heterosubtypic influenza infection by altering the antibody repertoire generated during the primary infection.

Rapamycin reduces class-switching and germinal centers

To determine how rapamycin alters antibody synthesis during influenza virus infection, we analyzed the serum from rapamycin or PBS-treated, HKx31-infected mice by the standard hemagglutination inhibition (HI) and virus microneutralization assays. The HI assay measures the capacity of serum antibodies to neutralize the virus by inhibiting the interaction between the HA of influenza and the sialic acid receptor on red blood cells[28]. The HI titer against HKx31 virus did not differ significantly between mice treated with rapamycin or PBS, and it was negligible against ΔVn1203 virus for both groups (Table 1). Microneutralization of infectivity is more sensitive than the HI assay, and is generally thought to reflect the capacity to inhibit viral entry and replication. Again, the neutralization titers for HKx31 virus were similar for both groups. In addition, we detected weak neutralization of ΔVn1203 virus in both PBS and rapamycin-treated serum, though this was only apparent at very high concentrations and was similar for both groups. Even so, while we did not detect significant amounts of neutralizing antibody specific for ΔVn1203 virus, other data indicate that non-neutralizing antibodies that bind to internal and external influenza epitopes may also provide protection during an influenza virus infection[13]. To probe this possibility, we next determined antibody titers for HKx31 or ΔVn1203 epitopes by ELISA, using whole virus bound to plates to give access to both external and internal viral epitopes. Unexpectedly, the concentration of HKx31-specific IgM antibody was significantly increased in the rapamycin-treated mice compared to the controls, while

HKx31-specific IgG was moderately decreased (Fig. 7a,b). As expected, cross-reactive antibodies binding ΔVn1203 epitopes in both groups of mice were not as prevalent as those specific for HKx31 epitopes (Fig. 7b,c), and the amount of IgM cross-reactive with ΔVn1203 epitopes was below the amount of detection by ELISA (data not shown). While the total amount of IgG specific for ΔVn1203 epitopes did not differ between the groups (Fig. 7c), the concentrations were close to the limit of detection.

The increase in influenza-specific IgM and decrease of IgG antibody concentrations in rapamycin-treated mice (Fig. 7a) suggests that rapamycin may alter the antibody repertoire by inhibiting antibody class-switching. Consequently, we measured the different classes of antibodies present in the serum of mice 28 days after infection with the HKx31 virus with and without rapmycin. In control mice, HKx31 infection increased the amount of serum IgM, IgG1, and IgG2b compared to naïve controls. However, only IgM increased in the rapamycin-treated mice (Fig. 8a). These data support the observation that rapamycin treatment does not prevent the generation of influenza-specific antibodies, although it decreases the generation of class-switched antibodies.

Antibody class-switching involves proliferation of B cells and the formation of germinal centers after antigen exposure[29]. Thus, we next investigated whether rapamycin inhibited the formation of germinal centers induced by HKx31 infection. When analyzed 15 days following HKx31 priming, the proportion and number of germinal center ($GL7^+$) B cells in the mediastinal lymph node (MLN) that drains the peritoneal cavity, were significantly decreased in rapamycin-treated mice compared to PBS-treated controls (Fig. 8b and Supplemental Fig. 7a). Moreover, staining of sections with Bcl-6 and PNA established that germinal centers were indeed absent from the MLNs of these rapamycin-treated mice (Fig. 8c,d and data not shown). In the spleen, the numbers of germinal centers were not significantly different in HKx31-infected or naïve mice for either the rapamycin or PBS-treated groups (Supplemental Fig. 7b). These data indicate that rapamycin inhibits the formation of germinal centers in the draining lymph nodes following primary HKx31 infection.

To examine whether B cell proliferation was blocked by the dose of rapamycin used in these experiments, we analyzed the number of B cells that incorporated BrdU during a 4-h pulse. Fewer $BrdU^+$ B cells were found in the lymph nodes of rapamycin-treated versus control mice at 15 days following HKx31 infection (Fig. 8e and Supplemental Fig. 7c). However, this dose of rapamycin did not completely block B cell proliferation in the lymph nodes as evidenced by similar proportions of $GL7^+$ cells that incorporated BrdU in rapamycin and PBS-treated mice (Supplemental Fig. 7e). In the spleen, the number of $BrdU^+$ cells significantly decreased at day 20, as did the proportion of $GL7^+$ B cells that incorporated BrdU in rapamycin- compared to PBS-treated mice (Supplemental Fig. 7d,f). These data suggest that rapamycin modifies antibody generation by limiting B cell proliferation and germinal center formation.

Rapamycin inhibits class-switching independent of proliferation

To examine whether rapamycin inhibits antibody class-switching by decreasing proliferation, or by directly preventing antibody class-switching, we utilized an *in vitro*

assay to establish a dose of rapamycin low enough to not inhibit B cell proliferation, which enabled us to analyze class-switching independent of proliferation (Fig. 9a,b). The B cells were stimulated with LPS or LPS and IL-4 for 4 days with increasing amounts of rapamycin. The generation of $IgG2b^+$ and $IgG3^+$ B cells in response to LPS was inhibited at 0.5 ng/ml of rapamycin, although proliferation was intact (Fig. 9a–d). Likewise, in response to LPS and IL-4, the number of $IgG1^+$ and IgE^+ B cells decreased in the presence of rapamycin (Fig. 9e,f). In response to both stimuli, rapamycin increased the number of IgM^+ B cells demonstrating that rapamycin does not diminish B cell survival, but rather, inhibits the switch from IgM to the other antibody classes (Fig. 9g).

We next analyzed the induction of activation-induced cytidine deaminase (AID) 24 h after stimulation, a time before proliferation is affected by rapamycin (Fig. 9h), to confirm that the defect in class-switching in the presence of rapamycin is not due to inhibition of proliferation. AID is encoded by the gene, *Aicda*, and is absolutely required for class-switching[30]. As mTOR functions in two distinct signaling complexes, mTORC1 and mTORC2[14], we also tested *Aicda* induction in B cells with an inducible deletion of *Raptor*, an essential protein in the mTORC1 complex. *Raptor*-deficient ($Raptor^{fl/f}.Rosa26^{ERcreT2}$, $Raptor^{B-/-}$) and control ($Raptor^{+/+}.Rosa26^{ERcreT2}$, $Rosa26^{ERcreT2}$) mice, received injections of tamoxifen, i.p., for 4 consecutive days. Eight days after the last injection, IgM^+ B cells were harvested from spleens and stimulated *in vitro* for 24 hours with LPS and IL-4, with and without rapamycin. The numbers of control ($Rosa26^{ERcreT2}$), and *raptor*-deficient ($Raptor^{B-/-}$) B cells were similar, suggesting comparable proliferation at this time (Fig. 9i). Interestingly, *Aicda* mRNA increased significantly by 24 h in wild-type B cells, but not in B cells deficient in *raptor*, or in B cells treated with rapamycin (Fig. 9j). These results indicate that mTORC1, in particular, is required for *Aicda* transcription and subsequent class-switching. Moreover, the requirement for mTORC1 is observed prior to proliferation, and is not simply a consequence of reduced cell division. Together these data show that mTOR is important for B cell class-switching and germinal center formation, and that inhibiting this pathway with rapamycin during primary influenza virus infection alters antibody generation by preventing class-switching.

Rapamycin alters the antibody repertoire specificity

While IgM concentrations specific for HKx31 were higher for rapamycin treated mice, the IgG titers for HKx31 or ΔVn1203 were not significantly different between the PBS and rapamycin treated groups. However, the ELISA approach does not measure the antibody amounts specific for each epitope. A different approach is needed to determine whether rapamycin changes the antibody repertoire by modifying the frequency of antibodies specific for particular epitopes. To obtain a sample “footprint” of the overall Ig response during a primary infection, we evaluated the prevalence of antibodies specific for the HA proteins of HKx31 and ΔVn1203 viruses. Antigen microarrays were generated with peptides spanning the HKx31 and ΔVn1203 HA proteins. The peptides were 20 amino acids in length, with an overlap of 15 amino acids to offer a dense coverage of potential epitopes. Sera from mice infected with HKx31 virus and treated with rapamycin or PBS for 20 days were incubated on the arrays and the amount of IgG or IgM antibodies binding to each epitope was quantified by measuring the fluorescence intensity of bound anti-mouse IgM or

IgG. The increased sensitivity of this assay compared to ELISA allowed us to analyze both IgM and IgG specific for the HKx31 (H3) and ΔVn1203 (H1) HAs from 10 mice per group. We first tested the overall antibody response pattern to the ΔVn1203 HA. Interestingly, the response patterns of both IgM (Fig. 10a) and IgG (Fig. 10b) clustered separately into two distinct groups depending on the rapamycin treatment. This suggests that treatment with rapamycin induces a unique antibody signature.

We then identified the specific antigens for which the responses of the two groups significantly differed, focusing only on those antigens in which the overall response rates were greater than 20%. For each of these probes, we computed a Fisher's exact test on the number of responding mice in each of the two groups with separate analyses being made for HKx31 IgM (Fig. 10c), HKx31 IgG, (Fig. 10d), ΔVn1203 IgM (Fig. 10e), and ΔVn1203 IgG (Fig. 10f). The antigen sets showing statistically significant differences between the PBS and rapamycin-treated mice are depicted (Fig. 10c–f). In general, we found more diversity between the groups in the IgM antibodies compared to the IgG antibodies specific for each viral strain. This may be because the IgM repertoire is generally more diverse than the IgG repertoire. Analysis of antibodies specific for ΔVn1203 established the presence of unique IgM and IgG signatures specific for particular HA epitopes in both the PBS-treated and rapamycin-treated mice (Fig. 10e,f). These data show that rapamycin alters the repertoire of antibodies specific for influenza A virus HA glycoproteins.

We next investigated the location of the peptides yielding differential responses between PBS and rapamycin-treated mice in the HAs from HKx31 and ΔVn1203. The solved structure of HKx31 HA does not include the most c-terminal portion of the protein. Therefore, the peptide with a start position of 551 (Fig. 10c,d) is not on the structure. Nevertheless, this analysis highlights that antibody responses to several epitopes on the HKx31 HA found for the PBS-treated HKx31-primed mice were strikingly absent from the comparable rapamycin-treated group, suggesting that rapamycin decreased the overall HA-specific antibody response in the primary infection (Fig. 10g). Furthermore, the ΔVn1203 HA peptides bound by antibodies from the rapamycin-treated versus control mice are located on the exterior portion of ΔVn1203 HA, indicating that they may be accessible on the surface of the intact virus or virus-infected cell (Fig. 10h).

To further investigate the accessibility of these peptides, we computed solvent accessible surface areas (SASA) using both a water-sized probe (1.4Å) and a larger 4Å probe that would better mimic accessibility to antibodies. We found that all the peptides that induced an antibody response exclusively in the rapamycin-treated mice were surface accessible, unlike some of the specificities that were differentially observed in the PBS-treated mice (Supplementary Table I). Moreover, two of the peptides identified in the rapapmycin-treated mice are previously described antibody contact sites. Interestingly, one of the peptides unique to the rapamycin-treated set (Fig. 10f, start position 16) bound an epitope in the stem region of the ΔVn1203 HA, which is typically more conserved between different subtypes of HA, and could thus provide protection against multiple influenza subtypes. In summary, this analysis illustrates that rapamycin decreases the dominant antibody response to the HA of the vaccine strain, which in turn, allows antibodies specific for more conserved epitopes to become more prevalent. Taken together, our data suggest that, in addition to altering

antibody class profiles, rapamycin changes the antibody repertoire following vaccination, leading to enhanced protection against a lethal heterosubtypic infection.

Discussion

Here we describe a model where rapamycin treatment enhances protection against a lethal H5N1 influenza infection following vaccination with a relatively avirulent H3N2 influenza A virus. We took advantage of this system to investigate the components of the immune response that boost this cross-strain protection, and made several discoveries. Most notably, a broader antibody response, rather than a highly selected and affinity-matured repertoire enhances heterosubtypic immunity. This protective response is promoted by the use of rapapmycin to inhibit mTOR and reduce germinal center formation and immunoglobulin class-switching during primary infection. Importantly, the resultant altered antibody repertoire protects naïve mice against a lethal, heterosubtypic influenza A virus infections.

Rapamycin modified the antibody repertoire in two ways. First, it decreased antibody class-switching, thereby increasing the prevalence of influenza-specific IgM antibodies. While levels of cross-reactive, ΔVn1203-specific IgM antibodies were not measurable, the fact that total IgG, but not IgM concentrations were decreased in the rapamycin-treated mice implies that the proportion of IgM to IgG antibodies is greater in rapamycin-treated mice compared to PBS. Perhaps the pentameric IgM complexes enhance low affinity binding by increasing the avidity for a particular epitope. As antibodies specific for the conserved epitopes may bind with a lower affinity than those that bind the highly divergent HA epitopes, this increased avidity may be necessary for these cross-reactive antibodies to be effective[13]. Furthermore, IgM can directly activate the complement pathway to enhance protection by accelerating the clearance of virus particles and infected cells. Second, rapamycin altered the frequency of antibodies specific for particular influenza epitopes. This may have steered the immune response away from strain-specific responses to more cross-reactive responses. Although our antibody analysis is likely an underestimate of the true diversity given that the antigen arrays only measured the antibody response to HA, and may not have detected antibodies that bind tertiary protein conformation, we found that rapamycin modified the binding spectrum for antibodies generated during primary infection. If these altered specificities indeed provide protection, they offer possible strategies for developing therapeutics to protect individuals in the event of a deadly pandemic.

How might these cross-reactive antibodies enhance viral clearance? Rapamycin did not increase measurable neutralizing antibody titers in serum from mice infected with the HKx31 virus indicating that the cross-reactive antibodies protect by a means other than preventing virus entry into host cells, or fusion of the virus to the cell membrane. Though it is also possible that the available assays are not sensitive enough to measure weakly binding antibodies, or may lack other components of the immune system, such as complement, that operate in the whole animal. Other studies have demonstrated protection by cross-reactive influenza-specific antibodies that did not neutralize virus *in vitro*[13]. Antibodies can facilitate complement-mediated clearance of viral particles or infected cells[31,32], Fc receptor-mediated phagocytosis of viral particles[33], and antibody-dependent cell-mediated

cytotoxicity[11,34,35]. In addition, antibody/antigen complexes can activate dendritic cells to enhance antigen presentation and chemokine production[36].

Rapamycin disrupted the formation of germinal centers, which may in turn, have altered the antibody repertoire. During an immune response, antibodies undergo class-switching and affinity maturation in the germinal centers[29]. Over time, isotype-switched B cells that produce the highest affinity antibodies are selected for preferential expansion. For an influenza infection, the majority of these high affinity antibodies are specific for the globular head of the HA protein[13]. While these isotype-switched, affinity-matured antibodies provide the necessary protection to prevent reinfection with homologous strains, they may outcompete the lower affinity antibodies that are specific for epitopes conserved across different influenza subtypes. Our data suggest that rapamycin blocks the formation of germinal centers and high affinity antibodies. Consequently, lower affinity antibodies with a greater potential to be cross-reactive are not outcompeted, and therefore become more prevalent.

Our data also show that mTOR plays a critical role in forming germinal centers and antibody class-switching. As B cell proliferation, germinal center formation, and antibody class-switching are so intimately linked, it is difficult to say definitively at which stage mTOR is required. Clearly, mTOR is needed for B cell proliferation both *in vitro* and *in vivo*[37]. However, our data indicate that, at a low dose of rapamycin, which did not block proliferation, antibody class-switching and the induction of *Aicda* were inhibited, indicating that mTOR is critical for class-switching independent of proliferation. Moreover, rapamycin and the deletion of *Raptor* inhibited the induction of *Aicda* within 24 hours of stimulation, yet proliferation in the rapamycin and control-treated samples was comparable.

In addition, rapamycin may impede germinal center formation by blocking the survival of germinal center B cells. Germinal center B cells are highly susceptible to apoptosis and are therefore dependent on mTOR-induced anti-apoptotic proteins, such as Mcl-1, for survival[29]. Another likely mTOR-dependent step is the migration of B cells and T cells to chemokines that are important for establishing the germinal centers. CXCR4 on B cells is required for germinal center formation, and migration to the ligand, SDF-1, is dependent on mTOR[38,39]. Based on these data and our findings, we propose that rapamycin blocks the proliferation, survival, and migration of B cells, all of which contribute to the absence of germinal centers in rapamycin-treated mice.

The T follicular helper (T_{fh}) cells play an essential role in germinal center formation and the selection of affinity-matured antibodies[40]. Our data do not exclude the possibility that rapamycin alters $CD4^+$ T_{fh} cells or dendritic cells, which in turn affects germinal center formation. In fact, we did find a reduction in T_{fh} numbers following HKx31 infection of rapamycin-treated mice compared to controls (data not shown). However, the fact that deletion of *raptor* in B cells or rapamycin treatment *in vitro* blocked induction of *Aicda* transcription, proliferation, and antibody class-switching in a B cell-intrinsic manner indicates that mTORC1 plays a critical role directly in B cells regulating proliferation and antibody class-switching. In addition, $CD4^+$ T cells were required for the rapamycin-mediated protection, but germinal centers were absent, which indicates that $CD4^+$ T cells

play other necessary roles in antibody formation, including activating the B cells or cytokine secretion.

Overall, our data demonstrate that mTORC1 is required for B cell class-switching and germinal center formation. Inhibition of this pathway during influenza vaccination promotes a unique antibody repertoire, which enhances heterosubtypic immunity to influenza infection, and has important implications for identifying novel cross-reactive antibodies. Moreover, this approach could be extended to vaccine design against other viruses, which would benefit from cross-reactive antibodies such as HIV.

Methods

Mice

Female 8–10-week old C57BL/6J and B cell-deficient mice homozygous for the *Ighm*^{tm1Cgn} mice targeted mutation (μMT mice) were purchased from The Jackson Laboratory. *Raptor*$^{fl/fl}$ *Rosa26*^{ERcreT2} mice were a generous gift from H. Zeng (). Mice were held under specific pathogen-free conditions at St. Jude Children's Research Hospital. Animal studies met the approval of the Animal Ethics Committee.

Viruses and infection

The HKx31 and ΔVn1203 viruses were constructed using the eight-plasmid reverse genetics system[41] containing the six internal genes of A/Puerto Rico/8/34 (PR8) and HA and NA surface proteins from either A/HKx31 (H3N2) or A/Vietnam/1203/04 (H5N1), respectively. The mutant HKx31 virus lacking the dominant CD8$^+$ T cell epitopes (ΔCD8-x31) was previously described[27].

For prime/challenge infection protocols, mice were primed i.p. with 10^8 egg 50% infective dose (EID_{50}) units of HKx31 virus or ΔCD8-x31 virus. Four weeks later, mice were anesthetized with Avertin (2,2,2-tribromethanol) and challenged i.n. with 4.5 x 10^5 EID_{50} of ΔVn1203 or 2 x 10^4 pfu of Sendai virus. In serum transfer experiments, μMT mice received 4 x 10^4 EID_{50} of ΔVn1203 the day after serum transfer. Mice were weighed and monitored for clinical signs of disease daily. Mice that were determined to be moribund based on a body-index score were euthanized. Rapamycin (Rapamune, Wyeth) diluted in PBS was administered at 75 μg/kg of body weight via a daily i.p. injection.

T cell depletion

Mice were injected i.p. with 100 μg anti-CD4 (clone GK1.5), anti-CD8α (clone 53-6.7), or rat IgG2b, κ isotype-control (RTK4530) antibodies (Biolegend) on days indicated in figure legends.

Organ removal and Flow cytometric analysis

Mice were euthanized by CO_2 asphyxiation. Bronchoaleveolar lavage cells were extracted. Lung, spleen, and mediastinal lymph node (MLN) were then excised. Cells were incubated with anti-CD16/CD32 and stained with antibodies for CD8α (53-6.7), CD4 (RM4-5), B220 (RA3-6B2), KLRG1 (2F1), CD127 (A7R34), IgE (23G3) from eBiosciences, IgG1

(RMG1-1; Biolegend), IgM (RMM-1; BioLegend), IgG2b (γ2b; Invitrogen), IgG3 (polyclonal; AbD serotec), GL7 (GL7; BD Biosciences). For tetramer staining, cells were incubated 60 min at 25 °C with tetramer specific for the H-2D^b NP_{366} or H-2D^bPA_{224} epitopes, followed by staining with surface antigens. Regulatory T cells were identified using the Foxp3 (FJK-16s; eBioscience) kit, according to manufacturer's recommendations. Flow cytometry data were acquired on an upgraded five-color FACScan, FACScaliber, or LSRII (Becton Dickinson) and analyzed with FlowJo software (TreeStar). For histology, spleens and MLN were fixed in 4% formaldehyde, embedded in paraffin, and stained with hematoxylin, eosin, and Bcl6.

Plaque Assay

Harvested lungs were stored at −80 °C prior to use. Madin-Darby canine kidney (MDCK) cells were plated in six-well plates and infected with serial dilutions of 1 ml of homogenized lung supernatant. Infected monolayers were incubated at 37 °C for 1 h and washed with PBS. The cells were overlayed with 0.8% agarose in minimal essential medium containing 1 mg/ml trypsin and at 37 °C for 72 h. The agar was removed and monolayers were stained with crystal violet to visualize plaques.

Ag-specific ELISA

Microtiter plates (Nunc) were coated with purified whole influenza HKx31 virus or ΔVn1203 virus in PBS overnight at 4 °C, washed and incubated with serum for 2 h[42]. Plates were washed and influenza-specific IgG was detected using goat anti-mouse IgG alkaline phosphatase conjugate (Southern Biotechnology Associates). P-nitrophenyl phosphate (Sigma-Aldrich) was added for 90 min at 25 °C and optical density values were determined at 405 nm in a microplate reader (Molecular Devices).

Detection of serum Ig

Serum Ig was measured using a Milliplex® MAP kit (Millipore Corporation) according to manufacturer's instructions.

Bromodeoxyuridine incorporation

HKx31-infected and naïve mice received two i.p. injections of BrdU (1.0 mg/ml) 4 h and 2 h prior to harvest. Spleen and MLN were stained with anti-BrdU using the BrdU kit from BD Biosciences, according to the manufacturer's instructions.

Antigen microarrays

Twenty amino acid peptides spanning the HA of HKx31 and ΔVn1203 were generated with 15 amino acids overlap. For each strain, 111 peptides were synthesized with a MultiPep RS (IntavisAG) peptide synthesizer using a modified SPOT synthesis protocol[43,44]. The peptides were lyophilized in a 384-well microtiter plate and stored at −20 °C.

Peptides were resuspended in 12.5 μl DMSO and 12.5 μl of ultra-pure water to create a working solution of approximately 1 mg/ml. Peptide stocks were diluted 1:4 in protein printing buffer (3X Saline Sodium Citrate, 0.1% Polyvinyl Alcohol, and 0.05% Tween 20). Peptide integrity was confirmed using positive controls, hemagglutinin A (HA)

(YPYDVPDYA) and FLAG (DYKDDDDK), in multiple replicate wells for optimization of array printing conditions.

Peptides were printed in triplicate, on N-hydroxysuccinimide ester derivatized glass slides (H slides, Schott/Nexterion AG) using a Microgrid-II microarrayer (Biorobotics) with contact microarray pins (SMP4B, TeleChem). During printing, relative humidity was maintained at ~50%. Following printing, a secondary immobilization step was carried out at 100% relative humidity for 1 h. Arrays were stored at −20°C.

Printed grids were outlined with a PAP hydrophobic pen (Research Products International Corp). Serum samples were diluted 1:20 in 1% BSA, incubated on slides for 2 h in a humidified chamber at 25 °C, then washed twice with PBS-T, once with PBS, and once in deionized water. Bound immunoglobulins were detected with Alexa Flour 647-goat anti-mouse IgG and Dylight 549-goat anti-mouse IgM (Jackson ImmunoResearch) for 45 min. Arrays were washed as above and spin-dried at 2000 *g* for 5 min.

Slides were scanned on a 2-laser GenePix 4100 scanner (Molecular Devices) probing for IgM and IgG simultaneously. Images were analyzed by GenePix version 6.1 to obtain the mean fluorescence intensity (MFI) for each probe. All samples were run the same day and processed together. Negative controls were run in triplicates for background subtraction. Background subtracted responses below 1000 MFI were considered negative (MFI range from 0–65,000). All subsequent data analysis was performed in Matlab (Mathworks). For each probe, we used the median response and subtracted the average background of multiple negative controls.

To analyze clustering of antibody signature profiles, the responses to the 110 peptides of ΔVn1203 HA was used to define a response vector for each mouse. Response vectors were compared using the Spearman rank-order correlation measure to create a 20x20 similarity matrix, in which each entry measures the similarity between a pair of response vectors, from a single mouse. The samples were clustered using complete-linkage, a hierarchical, unsupervised technique for clustering data points[45].

To compare response rates for specific antigens of each HA, we filtered the set of antigens in a treatment-blinded manner, removing all antigens with an overall response rate less than 20%. The remaining antigens were then tested for differences using Fisher's exact test. Antigens with P values <0.05 were reported. To adjust for multiplicity, we computed q-values adjusted for the False Discovery Rate. Due to the small sample size, family-wise error correction was not applied.

Protein structure analysis

Peptide solvent accessible surface areas were calculated using Rosetta software package[46], using a standard water-sized (1.4Å) probe and a larger 4Å probe to mimic accessibility to protein moieties. To make the surface areas more directly comparable, the large-probe accessible surface was projected back onto a 1.4Å shell before calculating the total area. Antibody contacting peptide residues were defined as HA positions having a heavy atom-

heavy atom distance less than 6Å to an antibody chain in any one of the following PDB structures: 1eo8, 1ken, 1qfu, 3gbn, 3lzf, 3sdy, 3sm5, 3ztj, 3ztn, 4fqi, 4fqv, 4fqy, or 4gms.

In vitro class switching assay

Splenic IgM^+ B cells were harvested using anti-mouse IgM magnetic beads (Miltenyi Biotec) and labeled with 0.5 μM carboxyfluorescein succinimidyl ester (CFSE). Cells were cultured in triplicate in 96-well plates at 0.7 x 10^5 cells per well in RPMI-1640 media (Gibco) supplemented with 2 mM L-glutamine, 50 μM 2-ME, 10% FCS, 5 mM HEPES, pH 7.2, 50 μg/ml penicillin/streptomycin, and, 50 μg/ml gentamicin. Cells were plated with media alone, *Eschericia coli* lipopolysaccharide (LPS) (50 μg/ml), or LPS and IL-4 (50 ng/ml) with rapamycin dilutions. Cells were incubated at 37 °C for 96 h, then stained with fluorescently labeled IgG1, IgE, IgM, IgG2b, and IgG3.

Aicda transcription

RNA was extracted from purified IgM^+ cells using the RNeasy® Mini Kit (Qiagen). First-strand complementary DNA was synthesized from 100 ng of total RNA using TaqMan® Reverse Transcription Reagents (Applied Biosystems). cDNA was analyzed in triplicate by SYBR Green dye (Thermo Scientific) using *Aicda* and *CD79b* primers[47] in an Applied Biosystems 7500 Fast Real-Time PCR System over 50 cycles (5 sec, 95°C; 30 sec, 60°C). *Aicda* transcript abundance was quantified using the relative standard curve method (Applied Biosystems, User Bulletin #2) and normalized to *CD79b* expression.

Hemagglutination inhibition and MDCK virus neutralization

Mouse sera were treated overnight with *Vibrio cholerae* receptor-destroying enzyme (Denka-Seiken), heat inactivated for 30 minutes at 56 °C, then assayed according to a standard hemagglutination-inhibition protocol[48] using 4 HA virus units. For the neutralization assay, heated serum was diluted serially in PBS, mixed with 100 EID_{50} of virus, incubated for 30 min at 4 °C, then incubated on MDCK monolayers at 37°C for 72 h. Virus that was not neutralized was detected by plaques.

Statistical analysis

Data were analyzed with GraphPad Prism 5.0 (GraphPad Software). Survival experiments were analyzed using the Kaplan-Meier survival probability estimates. Weight loss comparisons were made using unpaired *t* tests. Quantitative differences between two samples were compared with the Mann-Whitney *U* test. *P*-value < 0.05 was considered significant.

Supplementary Material

Refer to Web version on PubMed Central for supplementary material.

Acknowledgments

We thank H. Zeng (St. Jude) for help with the *Raptor*$^{fl/fl}$ *Rosa26* ^{ERcreT2} mice, B. Creasy and T. Oguin (both at St. Jude) for technical support, P. Vogel and the Veterinary Pathology Core at St. Jude for histology, S. Patrick and the staff of the Shared Animal Resource Center at St. Jude for animal husbandry. This project has been funded with

funds from the National Institute of Allergy and Infectious Diseases, National Institutes of Health, Department of Health and Human Services, under contract HHSN266200700005C and ALSAC.

References

1. Osterholm MT, Kelley NS. Mammalian-Transmissible H5N1 Influenza: Facts and Perspective. mBio. 2012; 3
2. Herfst S, et al. Airborne transmission of influenza A/H5N1 virus between ferrets. Science. 2012; 336:1534–1541. [PubMed: 22723413]
3. Imai M, et al. Experimental adaptation of an influenza H5 HA confers respiratory droplet transmission to a reassortant H5 HA/H1N1 virus in ferrets. Nature. 2012; 486:420–428. [PubMed: 22722205]
4. Pica N, Palese P. Toward a universal influenza virus vaccine: prospects and challenges. Annu Rev Med. 2013; 64:189–202. [PubMed: 23327522]
5. Thomas PG, Keating R, Hulse-Post DJ, Doherty PC. Cell-mediated protection in influenza infection. Emerging Infect Dis. 2006; 12:48–54. [PubMed: 16494717]
6. Okuno Y, Isegawa Y, Sasao F, Ueda S. A common neutralizing epitope conserved between the hemagglutinins of influenza A virus H1 and H2 strains. J Virol. 1993; 67:2552–2558. [PubMed: 7682624]
7. Throsby M, et al. Heterosubtypic Neutralizing Monoclonal Antibodies Cross-Protective against H5N1 and H1N1 Recovered from Human IgM^+ Memory B Cells. PLoS ONE. 2008; 3:e3942. [PubMed: 19079604]
8. Ekiert DC, et al. Cross-neutralization of influenza A viruses mediated by a single antibody loop. Nature. 2012; 489:526–532. [PubMed: 22982990]
9. Sui J, et al. Structural and functional bases for broad-spectrum neutralization of avian and human influenza A viruses. Nat Struct Mol Biol. 2009; 16:265–273. [PubMed: 19234466]
10. Corti D, et al. Heterosubtypic neutralizing antibodies are produced by individuals immunized with a seasonal influenza vaccine. J Clin Invest. 2010; 120:1663–1673. [PubMed: 20389023]
11. Corti D, et al. A neutralizing antibody selected from plasma cells that binds to group 1 and group 2 influenza A hemagglutinins. Science. 2011; 333:850–856. [PubMed: 21798894]
12. Wrammert J, et al. Broadly cross-reactive antibodies dominate the human B cell response against 2009 pandemic H1N1 influenza virus infection. J Exp Med. 2011; 208:181–193. [PubMed: 21220454]
13. Corti D, Lanzavecchia A. Broadly Neutralizing Antiviral Antibodies. Annu Rev Immunol. 201310.1146/annurev-immunol-032712-095916
14. Powell JD, Pollizzi KN, Heikamp EB, Horton MR. Regulation of immune responses by mTOR. Annu Rev Immunol. 2012; 30:39–68. [PubMed: 22136167]
15. Araki K, et al. mTOR regulates memory CD8 T-cell differentiation. Nature. 2009; 460:108–112. [PubMed: 19543266]
16. Pearce EL, et al. Enhancing CD8 T-cell memory by modulating fatty acid metabolism. Nature. 2009; 460:103–107. [PubMed: 19494812]
17. Turner AP, et al. Sirolimus enhances the magnitude and quality of viral-specific $CD8^+$ T-cell responses to vaccinia virus vaccination in rhesus macaques. Am J Transplant. 2011; 11:613–618. [PubMed: 21342450]
18. Wang Y, Wang XY, Subjeck JR, Shrikant PA, Kim HL. Temsirolimus, an mTOR inhibitor, enhances anti-tumour effects of heat shock protein cancer vaccines. Br J Cancer. 2011; 104:643–652. [PubMed: 21285988]
19. Rao RR, Li Q, Odunsi K, Shrikant PA. The mTOR kinase determines effector versus memory $CD8^+$ T cell fate by regulating the expression of transcription factors T-bet and Eomesodermin. Immunity. 2010; 32:67–78. [PubMed: 20060330]
20. Klenk HD, Garten W. Host cell proteases controlling virus pathogenicity. Trends Microbiol. 1994; 2:39–43. [PubMed: 8162439]

21. Venturi V, Davenport MP, Swan NG, Doherty PC, Kedzierska K. Consequences of suboptimal priming are apparent for low-avidity T-cell responses. Immunol Cell Biol. 2012; 90:216–223. [PubMed: 21556018]
22. Rutigliano JA, et al. Protective memory responses are modulated by priming events prior to challenge. J Virol. 2010; 84:1047–1056. [PubMed: 19889782]
23. Huber VC, Thomas PG, McCullers JA. A multi-valent vaccine approach that elicits broad immunity within an influenza subtype. Vaccine. 2009; 27:1192–1200. [PubMed: 19135117]
24. Belser JA, et al. Pathogenesis and transmission of avian influenza A (H7N9) virus in ferrets and mice. Nature. Jul 10.2013 10.1038/nature12391
25. Watanabe T, et al. Characterization of H7N9 influenza A viruses isolated from humans. Nature. Jul 10.2013 10.1038/nature12392
26. Zhou J, et al. Biological features of novel avian influenza A (H7N9) virus. Nature. 2013; 499:550–503.
27. Thomas PG, et al. Hidden epitopes emerge in secondary influenza virus-specific $CD8^+$ T cell responses. J Immunol. 2007; 178:3091–3098. [PubMed: 17312156]
28. Khurana S, Frasca D, Blomberg B, Golding H. AID activity in B cells strongly correlates with polyclonal antibody affinity maturation in-vivo following pandemic 2009-H1N1 vaccination in humans. PLoS Pathog. 2012; 8:e1002920. [PubMed: 23028320]
29. Victora GD, Nussenzweig MC. Germinal centers. Annu Rev Immunol. 2012; 30:429–457. [PubMed: 22224772]
30. Muramatsu M, et al. Class switch recombination and hypermutation require activation-induced cytidine deaminase (AID), a potential RNA editing enzyme. Cell. 2000; 102:553–563. [PubMed: 11007474]
31. Feng JQ, Mozdzanowska K, Gerhard W. Complement component C1q enhances the biological activity of influenza virus hemagglutinin-specific antibodies depending on their fine antigen specificity and heavy-chain isotype. J Virol. 2002; 76:1369–1378. [PubMed: 11773411]
32. Verbonitz MW, Ennis FA, Hicks JT, Albrecht P. Hemagglutinin-specific complement-dependent cytolytic antibody response to influenza infection. J Exp Med. 1978; 147:265–270. [PubMed: 627837]
33. Huber VC, Lynch JM, Bucher DJ, Le J, Metzger DW. Fc receptor-mediated phagocytosis makes a significant contribution to clearance of influenza virus infections. J Immunol. 2001; 166:7381–7388. [PubMed: 11390489]
34. Hashimoto G, Wright PF, Karzon DT. Antibody-dependent cell-mediated cytotoxicity against influenza virus-infected cells. J Infect Dis. 1983; 148:785–794. [PubMed: 6605395]
35. Jegaskanda S, et al. Cross-Reactive Influenza-Specific Antibody-Dependent Cellular Cytotoxicity Antibodies in the Absence of Neutralizing Antibodies. J Immunol. 2013; 190:1837–1848.10.4049/jimmunol.1201574 [PubMed: 23319732]
36. Nimmerjahn F, Ravetch JV. Fcgamma receptors as regulators of immune responses. Nat Rev Immunol. 2008; 8:34–47. [PubMed: 18064051]
37. Limon JJ, Fruman DA. Akt and mTOR in B Cell Activation and Differentiation. Front Immunol. 2012; 3:228. [PubMed: 22888331]
38. Allen CDC, et al. Germinal center dark and light zone organization is mediated by CXCR4 and CXCR5. Nat Immunol. 2004; 5:943–952. [PubMed: 15300245]
39. Zhang S, et al. Constitutive reductions in mTOR alter cell size, immune cell development, and antibody production. Blood. 2011; 117:1228–1238. [PubMed: 21079150]
40. Crotty S. Follicular helper CD4 T cells (TFH). Annu Rev Immunol. 2011; 29:621–663. [PubMed: 21314428]
41. Hoffmann E, Krauss S, Perez D, Webby R, Webster RG. Eight-plasmid system for rapid generation of influenza virus vaccines. Vaccine. 2002; 20:3165–3170. [PubMed: 12163268]
42. Andreansky SS, et al. Consequences of immunodominant epitope deletion for minor influenza virus-specific $CD8^+$-T-cell responses. J Virol. 2005; 79:4329–4339. [PubMed: 15767433]

43. Hilpert K, Winkler DFH, Hancock REW. Peptide arrays on cellulose support: SPOT synthesis, a time and cost efficient method for synthesis of large numbers of peptides in a parallel and addressable fashion. Nat Protoc. 2007; 2:1333–1349. [PubMed: 17545971]

44. Winkler DFH, Hilpert K, Brandt O, Hancock REW. Synthesis of peptide arrays using SPOT-technology and the CelluSpots-method. Methods Mol Biol. 2009; 570:157–174. [PubMed: 19649591]

45. Duda, RO.; Hart, PE.; Stork, DG. Pattern Classification. Wiley-Interscience; 2000.

46. Leaver-Fay A, et al. ROSETTA3: an object-oriented software suite for the simulation and design of macromolecules. Meth Enzymol. 2011; 487:545–574. [PubMed: 21187238]

47. Pone EJ, et al. BCR-signalling synergizes with TLR-signalling for induction of AID and immunoglobulin class-switching through the non-canonical NF-κB pathway. Nat Commun. 2012; 3:767.10.1038/ncomms1769 [PubMed: 22473011]

48. Hoffmann E, Lipatov AS, Webby RJ, Govorkova EA, Webster RG. Role of specific hemagglutinin amino acids in the immunogenicity and protection of H5N1 influenza virus vaccines. Proc Natl Acad Sci USA. 2005; 102:12915–12920. [PubMed: 16118277]

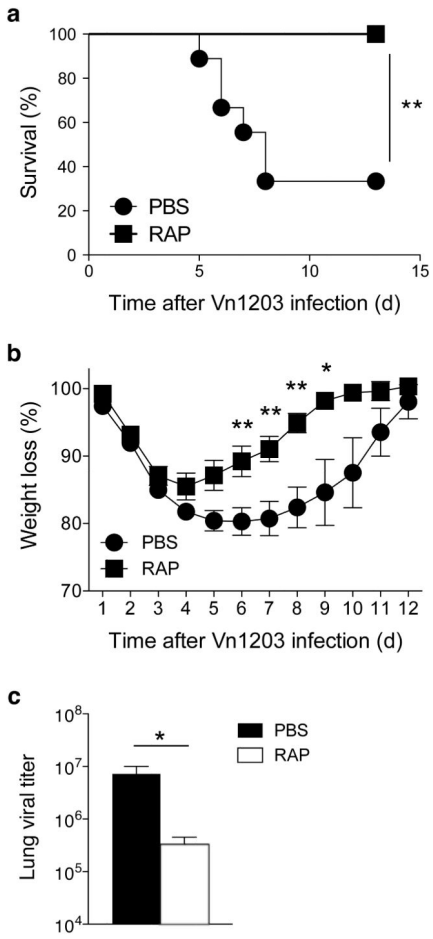

Figure 1.

Rapamycin treatment during primary infection decreases mortality following a lethal, heterosubtypic H5N1 secondary infection. (**a–c**) C57BL/6 mice received 75 μg/kg rapamycin or PBS, i.p. beginning 1 day prior to and daily for 28 days after primary infection with 10^8 EID_{50} of the H3N2 HKx31 i.p. On day 28, mice were challenged with 4.5 x 10^5 EID_{50} of the H5N1 ΔVn1203 i.n. and (**a**) monitored for survival (***P* = 0.003, Mantel-Cox test, *n* = 9 per group), and (**b**) weight loss. **P* < 0.05 and ***P* < 0.01, (unpaired *t* test). Data are representative of more than 10 separate experiments. (**c**) ΔVn1203 viral titers in the lung were determined by plaque assay 5 days after secondary infection. Data represent average viral titer ± s.e.m. (*n* = 5 per group; **P* = 0.040, Mann-Whitney *U* test). Data are representative of 6 independent experiments.

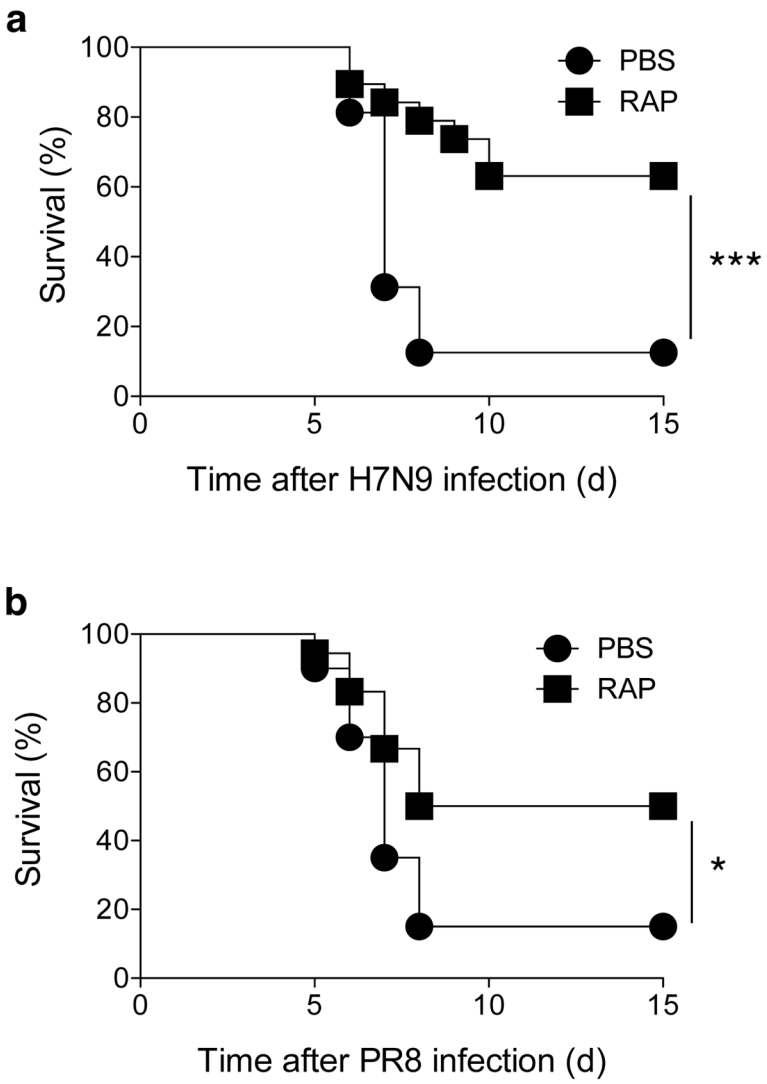

Figure 2.

Rapamycin protects mice from lethal H7N9 and H1N1 infections. Mice were infected with 10^8 EID_{50} of the H3N2 HKx31 i.p., treated with rapamycin daily, challenged i.n. on day 28 with (**a**) 4.5 x 10^5 EID_{50} of A/Anhui/1/2013 or (**b**) 4.5 x 10^5 EID_{50} of PR8 and monitored for survival (*P < 0.05 and ***P < 0.001, Mantel-Cox test, n = 16 and n = 18 per group, respectively). Data are a combination of 2 statistically significant independent experiments.

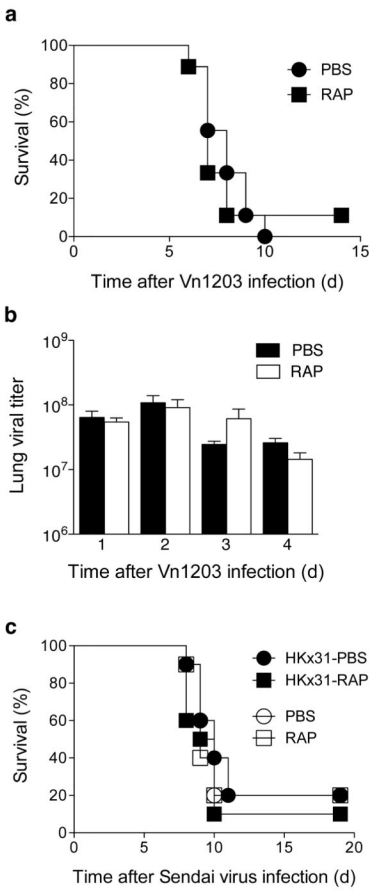

Figure 3.

Rapamycin-enhanced protection against lethal ΔVn1203 infection is influenza-specific and requires primary HKx31 infection. (**a**) Mice were treated with rapamycin or PBS for 28 days, infected with ΔVn1203 i.n., and monitored for survival (n = 9 per group; $P > 0.05$, Mantel-Cox test). (**b**) Mice were treated with rapamycin or PBS daily beginning 1 day prior to i.n. infection with 4 x 10^5 EID_{50} of ΔVn1203. Lungs were homogenized and virus titer was measured in a plaque assay. Results are expressed as the mean ± s.e.m. (n = 5 per group; $P > 0.05$, Mann-Whitney U test). (**c**) Mice were infected with HKx31 virus i.p., treated with rapamycin or PBS daily for 28 days and infected with 2 x 10^4 pfu of Sendai virus i.n. Control groups received PBS or rapamycin daily with no HKx31 primary infection (n = 10 per group; $P > 0.05$, Mantel-Cox test). Data represent 2 independent experiments.

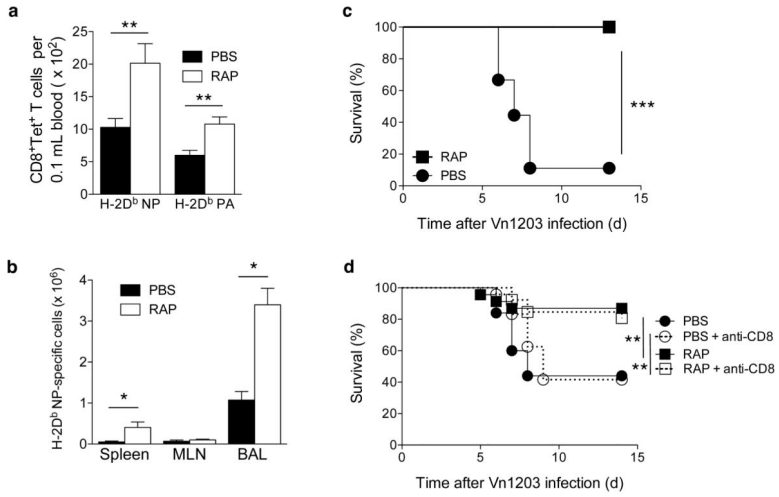

Figure 4.

Memory $CD8^+$ T cells are not required for rapamycin-mediated protection. **(ab)** Mice were injected with rapamycin or PBS and infected with HKx31 and ΔVn1203 as described in Fig. 1a. (**a**) On day 27, prior to secondary infection, a sample of blood from each mouse was analyzed for H-$2D^b$ NP_{366} and H-2Db PA_{224} tetramer binding. Data represent averages ± s.e.m. of 15 mice per group and are representative of 4 separate experiments (***P* < 0.01, Mann-Whitney *U* test). (**b**) Five days after secondary challenge with ΔVn1203, the spleen, MLN, and BAL were harvested and analyzed for D^bNP_{366} tetramer binding. Data represents the averages ± s.e.m. of 4 mice per group, which are representative of 4 separate experiments. (**P* < 0.05, Mann-Whitney *U* test). (**c**) Mice were infected with ΔCD8-HKx31 virus i.p., treated daily with rapamycin or PBS, and challenged with ΔVn1203 after 28 days and monitored for survival (*n* = 9 for PBS-treated mice, *n* = 15 for RAP-treated mice; ****P* < 0.001, Mantel-Cox test). Data are representative of 1 experiment. (**d**) $CD8^+$ T cells were depleted with anti-CD8 antibody (Clone 53-6.7) on days −3, −1, 1, 3, 5, and 17. Mice were infected with HKx31 virus, treated daily with rapamycin or PBS daily, and challenged with ΔVn1203 after 28 days. (*n* > 23 for each group; ***P* < 0.01 comparing PBS and RAP-treated wildtype mice and comparing PBS and RAP-treated, CD8-depleted mice, Mantel-Cox test). These data are a combination of 3 independent experiments.

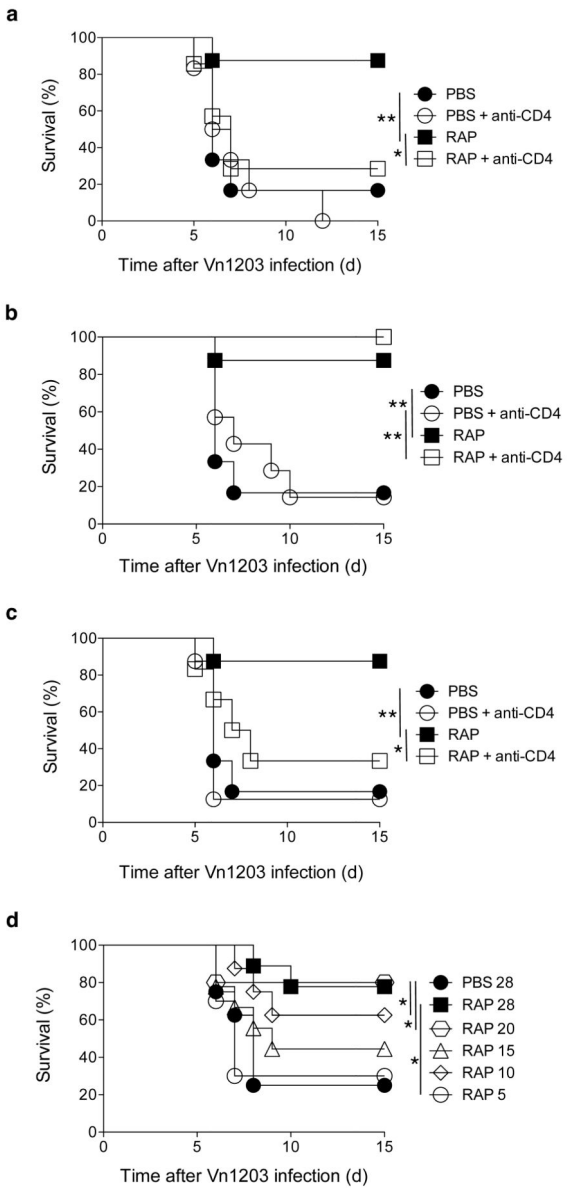

Figure 5.

$CD4^+$ T cells are required during primary HKx31 infection for rapamycin-mediated protection. (**a–c**) Mice were infected with HKx31, received rapamycin or PBS daily, and were challenged with ΔVn1203 as described in Fig. 1. $CD4^+$ T cells were depleted during the (**a**) primary and secondary infection by injection of anti-CD4 antibody (Clone GK1.5) −3, −1, 2, 5, 22, 24 days after HKx31 infection ($n > 6$ per group,) (**b**) during the secondary infection by injecting antibody 22 and 24 days after HK31 infection ($n > 6$ per group), and (**c**) during the primary infection by injecting antibody −3, −1, 2, 5 days after HKx31 infection ($n > 6$ per group). These data are representative of three independent experiments. (**d**) Mice were infected with HKx31 virus, received rapamycin or PBS daily for 5,10, 15, 20 or 28 days, and were then challenged with Δ Vn1203 virus 28 days following the primary HKx31 infection ($n > 8$ per group). *$P < 0.05$ and **$P < 0.01$, Mantel-Cox test. The 28 day

data are representative of more than 10 independent experiments. The 20, 15, 10 and 5 day data are representative of at least 2 independent experiments.

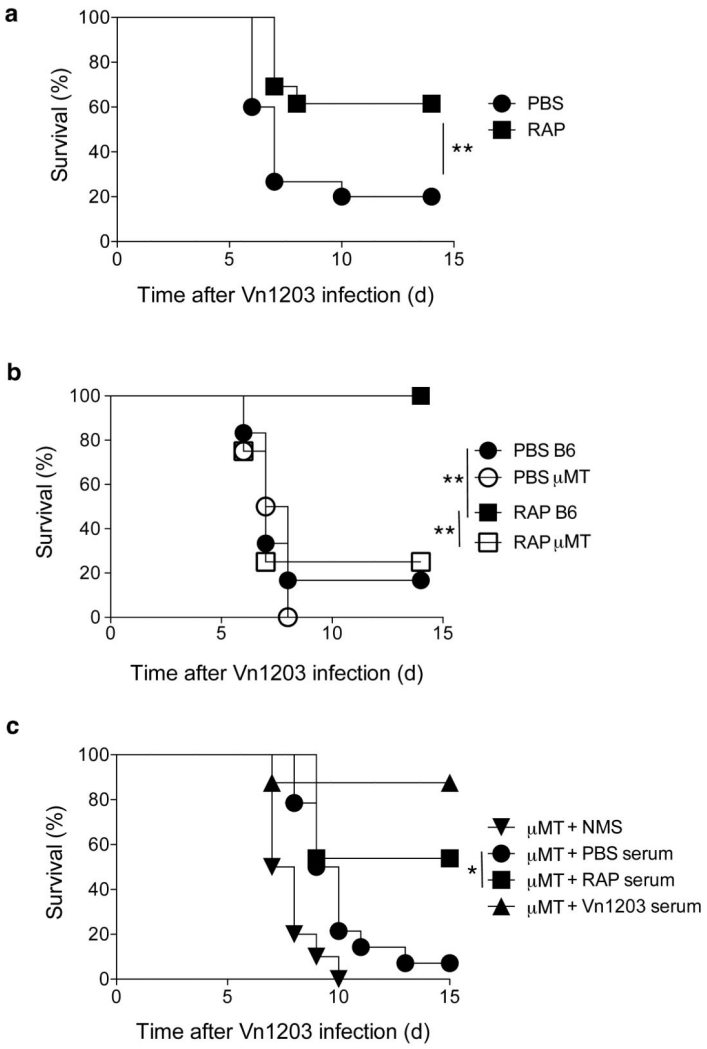

Figure 6.

B cells are required for rapamycin-mediated protection. (**a**) C57BL/6 mice were infected with HKx31 and received rapamycin or PBS daily for 28 days. Six weeks later, the mice were challenged with ΔVn1203 and monitored for survival. ($n > 13$ per group) (**b**) C57BL/6 and μMT mice were infected with HKx31, received rapamycin or PBS daily, and were challenged with ΔVn1203 ($n \geq 4$ per group). Data are representative of 2 independent experiments (**c**) One day prior to infection with 4 x 10^4 EID_{50} of ΔVn1203, μMT mice received 450 μl of serum i.p. from HKx31-infected mice treated with PBS ($n = 14$) or rapamycin ($n = 13$). Control mice received normal mouse serum ($n = 10$) or serum from ΔVn1203-infected mice ($n = 8$). The data are combined from 2 independent experiments *$P < 0.05$ and **$P < 0.01$, Mantel-Cox test.

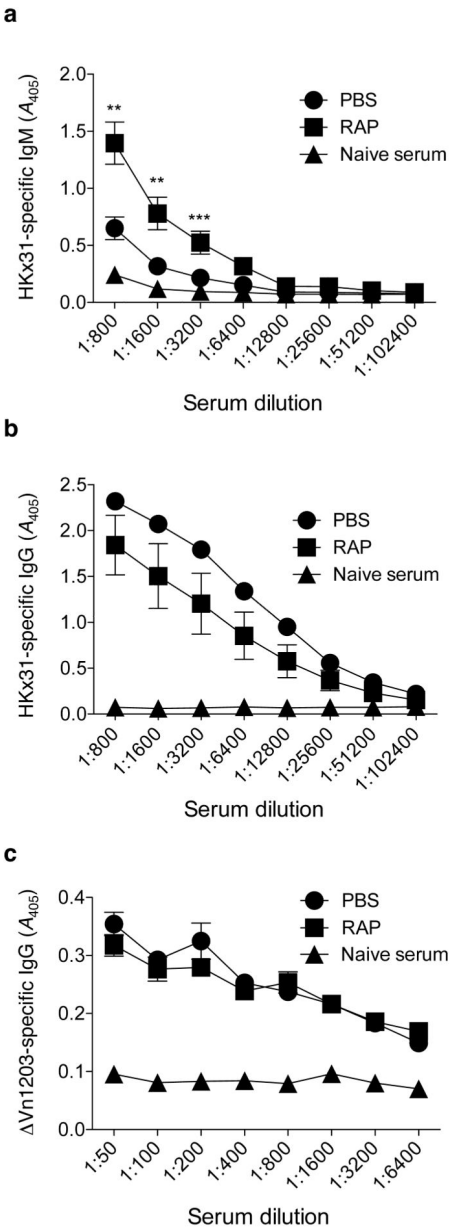

Figure 7.

Rapamycin-treated mice show elevated influenza-specific IgM antibodies. Mice were infected with HKx31 and received rapamycin or PBS daily as described in Fig. 1. On day 27, serum isolated from each mouse was analyzed by ELISA for (**a**) IgM specific for HKx31 ($n = 8$; $^{**}P < 0.01$ and $^{***}P < 0.001$, Mann-Whitney U test) (**b**) IgG specific for HKx31 ($n = 3$), (**c**) IgG specific for ΔVn1203 ($n = 4$). Each absorbance curve represents 5 independent experiments.

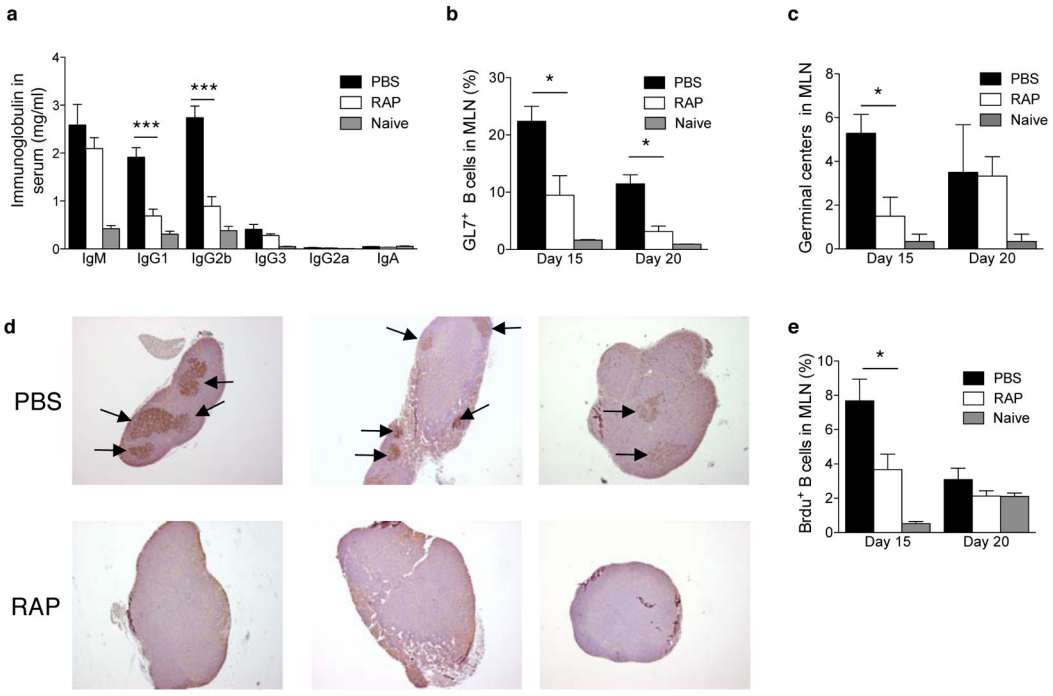

Figure 8.

Rapamycin decreases germinal center formation and reduces B cell class-switching. (**a**) Sera from mice infected with HKx31 and treated with rapamycin or PBS for 25 days were analyzed for Ig subtypes with a Milliplex Immunologlobulin Isotyping Panel (*n*=10). Data are representative of two independent experiments (**b**) MLN cells recovered 15 or 20 days after HKx31 infection and daily rapamycin or PBS injections were stained with antibodies to B220 and GL7. Each bar represents the average percent $GL7^+$ of $B220^+$ cells ± s.e.m. (*n* = 5,). Data are representative of 2 independent experiments. (**c**) Sections of MLN recovered 15 or 20 days after HKx31 infection and daily rapamycin or PBS injections were stained with Bcl-6 and PNA (data not shown) to identify germinal centers. The average number of germinal centers per section was calculated (*n* = 9 for day 15 and *n* = 3 for day 20). (**d**) Representative pictures of day 15 lymph nodes with arrows indicating germinal centers. (**e**) Fifteen and 20 days after primary infection, mice received a BrdU pulse 4 hours prior to harvest, and a second pulse 2 hours prior to harvest. The average percent ± s.e.m. of $B220^+$ cells in the MLN incorporating BrdU is shown (*n* = 5). **P* > 0.05 and ****P* > 0.001, Mann-Whitney *U* test.

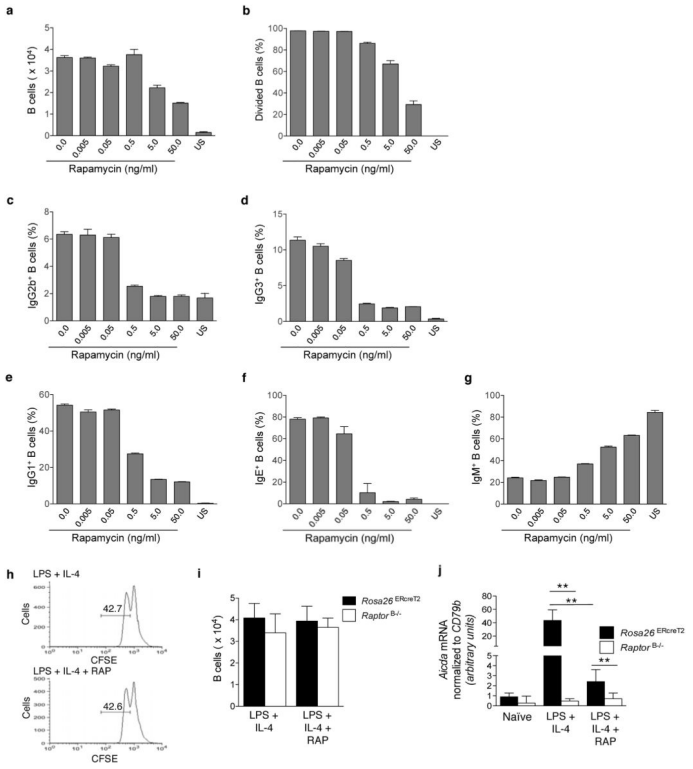

Figure 9.

mTORC1 is required for *Aicda* transcription and B cell class-switching. **(a–g)** IgM$^+$ B cells were enriched from the spleen, CFSE labeled, and left unstimulated (US) or stimulated *in vitro* for 4 days with (**a–d**) LPS or (**e–g**) LPS and IL-4 in the presence of increasing doses of rapamycin. (**a**) Shown is the average number ± s.d. and (**b**) the percent ± s.d. of live divided B cells. The proportion of live B cells that are positive for (**c**) IgG2b, (**d**) IgG3, (**e**) IgG1 (**f**) IgE, and (**g**) IgM is shown. These data are representative of 5 separate experiments. (**h–j**) Control *Rosa26*$^{\mathrm{ERcreT}}$ and *Raptor*$^{\mathrm{B-/-}}$ mice received injections of tamoxifen, i.p. daily for 4 days. Eight days after the last injection, IgM$^+$ B cells were harvested from spleens, stimulated for 24 hours with LPS and IL-4, with or without 0.5 ng/ml of rapamycin. (**h**) CFSE profile of control cells and (**i**) cell counts 24 hours after stimulation. (**j**) RNA was extracted and analyzed by qPCR for the level of *Aicda* transcripts relative to *Cd79b* transcripts. Data is a combination of 6 technical replicates and is representative of three biological replicates. (**P = 0.01, Mann-Whitney U test).

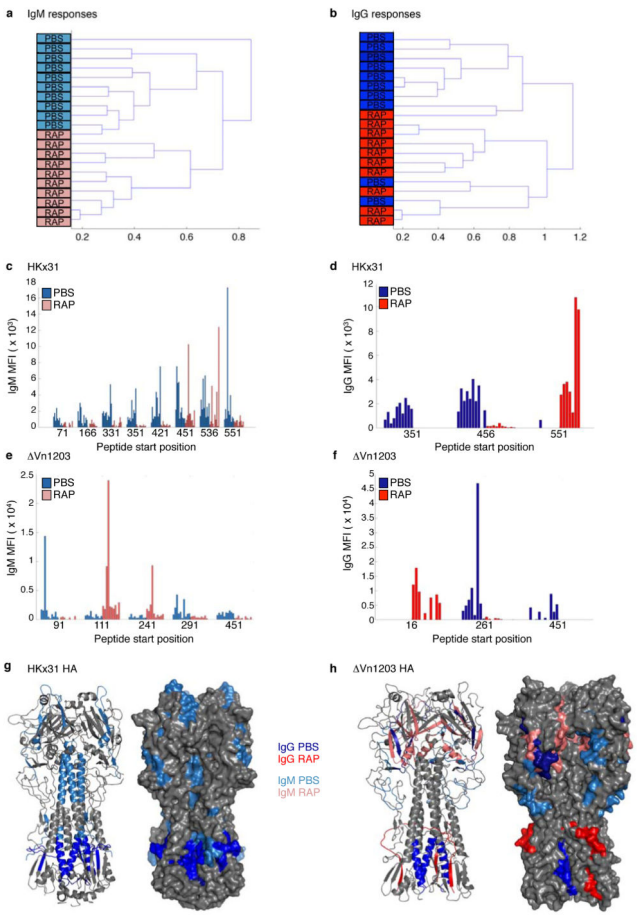

Figure 10.

Rapamycin modifies the antibody repertoire. Antigen microarrays were spotted with overlapping peptides that span the HA protein of both HKx31 and ΔVn1203. These were used to probe the IgM and IgG repertoire simultaneously using sera from animals sampled at 20 days following primary infection. Responses of 10 mice from each group were analyzed. (**a–b**) Samples were clustered using complete-linkage and the similarity between response patterns was defined as one minus the Spearman correlation coefficient between these vectors. Clustering dendrograms of response patterns of (**a**) IgM and (**b**) IgG to ΔVn1203 are depicted. (**c–f**) Specific antigens in which the responses between the rapamycin and PBS-treated mice had a $p < 0.05$ (Fisher's exact test) are shown. (**c**) IgM specific for HKx31 (**d**) IgG specific for HKx31 (**e**) IgM specific for ΔVn1203 (**f**) IgM specific for ΔVn1203. (**g–h**) The positions of the antigens described in (**c–f**) are imposed on the structure of (**g**) HKx31 HA and (**h**) Δ Vn1203 HA.

Table I

Serological cross-reactivity after infection with HKx31virus

Rapamycin does not increase the amount of neutralizing antibodies to HKx31 or ΔVn1203. Mice were infected with HKx31 virus and received rapamycin or PBS daily as described in Fig. 1. On day 27, plasma isolated from each mouse was analyzed in a hemagglutination inhibition assay and a micro neutralization assay as described in the methods.

	Against Vn1203		Against HKx31	
Serological test	**PBS serum**	**RAP serum**	**PBS serum**	**RAP serum**
Hemagglutination inhibition	0/11	0/12	7/7 (1:663 average titer)	8/8 (1:640 average titer)
Microneutralization	2/8 (1:5 average titer)	2/9 (1:5 average titer)	9/9 (1:324 average titer)	6/8 (1:198 average titer)